Science and Technology Indonesia
e-ISSN:2580-4391 *p*-ISSN:2580-4405
Vol. 9, No. 2, April 2024

Research Paper

ZnAl LDH-based Derivative Materials as Photocatalysts: Synthesis, Characterization, and Catalytic Performance in Tetracycline Degradation

Rohmatullaili[1,2*], Nur Ahmad[1,4], Desti Erviana[2], Zultriana[2], Dila Savira[2], Risfidian Mohadi[1,4], Aldes Lesbani[1,3,4]

[1]*Doctoral Program, Faculty of Mathematics and Natural Sciences, Universitas Sriwijaya, Palembang, 30139, Indonesia*
[2]*Department of Chemistry, Faculty of Science and Technology, UIN Raden Fatah Palembang, Palembang, 30252, Indonesia*
[3]*Magister of Material Science, Graduate Program, Universitas Sriwijaya, Palembang, 30139, Indonesia*
[4]*Research Center of Inorganic Materials and Complexes, Universitas Sriwijaya, Palembang, 30139, Indonesia*
***Corresponding author**: rohmatullaili_uin@radenfatah.ac.id

Abstract
Layered Double Hydroxide (LDH)-derived materials exhibited different characteristics from LDH precursors. The conversion of ZnAl LDH into its derivative material has been carried out to find the best catalyst for TC degradation. ZnAl (LDH)-based catalysts in this study have been effectively synthesized using coprecipitation, calcination, and restacking procedures. ZnAl Layered Double Oxide (LDO) is derived from the calcination of ZnAl LDH at 500°C. ZnAl LDH was also modified by adding *Garcinia mangostana* pericarp extract (GME). XRD, FT-IR, UV-DRS, and SEM-EDX were used to investigate the synthesized catalyst. ZnAl LDH exhibited the typical LDH FT-IR spectra, whereas ZnAl LDO showed metal oxide-like spectra, and the ZnAl-GME composite displayed the combination spectra of precursor material. The ZnAl LDH XRD diffraction pattern exhibited the attributes of a layered material, whereas the other three catalysts did not. Calcination destroyed the layered structure of ZnAl LDH, whereas the addition of GME to LDH and LDO generated a single-layered composite. The modified ZnAl-GME composite showed a decrease in both particle size and bandgap energy. At an ideal pH of 5, the synthesized catalyst was used in a batch system photodegradation of 5 mg/L Tetracycline (TC), employing solar light irradiation. ZnAl LDO holds the most significant catalytic activity and structural stability through the fifth regeneration cycle, degraded TC up to 100% in 90 minutes.

Keywords
LDH, LDO, Tetracycline, Photodegradation, *Garcinia mangostana*

Received: 5 January 2024, Accepted: 19 March 2024
https://doi.org/10.26554/sti.2024.9.2.457-469

1. INTRODUCTION

Pharmaceutical waste, classified as persistent organic pollutants (POPs), is a significant contributor to the current issue of water pollution. Tetracycline (TC) is among the pharmaceuticals recently found in water on an extensive level (Xu et al., 2023b). TC is a highly efficient antibacterial agent in humans and animals, among the most widely used antibiotics worldwide (Ajiboye et al., 2023). Non-biodegradable TC in water leads to residue formation that may enter the human food chain. Consequently, human bacterial resistance may develop, leading to more severe consequences over an extended period (Ahmed et al., 2023).

It is necessary to deal with wastewater treatment to ensure clean water availability. This action is required to accomplish one of the strategies outlined in the Sustainable Development Goals (SDGs) (Rohmatullaili et al., 2024). Waters containing TC have been treated using various techniques, such as coagulation, adsorption, sonocatalytic, advanced oxidation processes (AOP), and photocatalytic degradation (Li et al., 2023d). Photodegradation is the most promising method in wastewater treatment, with advantages such as being environmentally friendly, low energy and cost consumption, and sustainable method (Vasseghian et al., 2023; Wang et al., 2023a; Wang et al., 2022b). The utilization of an appropriate photocatalyst is a crucial factor that significantly influences photodegradation efficiency.

Photocatalysts are usually identical to transition metal oxides, which have proven to degrade antibiotics effectively (Vasseghian et al., 2023). Layered Double Hydroxide (LDH)-based materials have gained interest recently due to its photocatalytic capabilities (Azalok et al., 2021; Gholami et al., 2020). Ca/Fe-LDH-Na Alginate (Abed and Faisal, 2023), Mg-Al-LDH/AC nanocomposite (Asadpour et al., 2023), and NiCoMn-LDH (Devi et al., 2023) have been mentioned as photocatalysts in the TC degradation. LDH

holds a two-dimensional structure constructed from laminated materials. Its formula is typically represented as $[M^{2+}_{1-x}M^{3+}_{x}(OH)_2](An^-)_{x/n}.mH_2O$. Different chemical precursors affect the metal layer and anion interlayer composition. A high-performance catalyst with a large anion exchange capacity, broad surface area, and flexible component variation characterizes LDH (Aladpoosh and Montazer, 2022; Vasseghian et al., 2023; Yang et al., 2022). By inducing electron migration from the valence band to the conduction band via light irradiation, LDH is capable of producing holes with high oxidative potential (Vasseghian et al., 2023).

LDH offers many benefits but has limitations, including poor acid stability, unstable aqueous solution structure, and a tendency to agglomerate (Mo et al., 2023). Modifying LDH may mitigate its limitations while enhancing its catalytic efficiency. Calcinating LDH to LDO at 500°C results in a material with a larger surface area and more active sites than pristine LDH (Mo et al., 2023; Yang et al., 2023). Generating LDH composites is a further modification. This prevents agglomeration, resulting in less large particles with more active sites (Ahmad et al., 2023b). Lee et al. (2024) discovered that the integration of NiAl-LDH with a Co-Ni-based metal-organic framework resulted in NiAl LDH nanocomposites. The Zn-CuCo LDH-graphene composite, synthesized by Gholami et al., has a reduced particle size compared to the pristine Zn-CuCo LDH (Gholami et al., 2023). Further investigations suggest that the agglomeration of catalysts could prevented by adding natural extracts (Prabhu et al., 2022b).

In recent years, the exploration of natural extracts in inorganic synthesis has attracted attention. This is an approach to the principles of green chemistry, which develops eco-friendly methods and uses less hazardous materials. Previous researchers have reported the use of raw natural extracts, including *Clitoria ternatea* flower extract (Prabhu et al., 2022a), *Citrus microcarpa* (Villegas-Fuentes et al., 2023), mango peel (Isnaeni et al., 2021), *Salvia rosmarinus* (Silva-Osuna et al., 2022), and *Myristica fragrans* fruit extract (Faisal et al., 2021). Modification using *Clitoria ternatea* flower extract on ZnAl LDH has been reported by Rohmatullaili et al. (2024), where the modified LDH showed changes in specific characteristics. The use of *Garcinia mangostana* (GM) pericarp extract has also been reported in the synthesis of gold nanoparticles (Xin Lee et al., 2016), ZnO nanomaterials (Cong et al., 2023), and modification of Zn_2SnO_4 materials (Angasa et al., 2020). The use of *Garcinia mangostana* (GM) pericarp extract in modifying LDH-based materials has never been reported before, as it is the novelty of this research.

A number of bioactive compounds in GM pericarp extract, such as phenolic compounds, flavonoids, benzophenones, and anthocyanins, could serve as capping agents and inhibit agglomeration of the material (Angasa et al., 2020; Samrot et al., 2022). The introduction of GM fruit peel extract affected the surface shape, optical properties, and photocatalytic activity of the octahedral Zn_2SnO_4 material (Angasa et al., 2020). On the other hand, GM is a typical fruit of the Malay Peninsula, including Indonesia. Its abundance makes GM pericarp waste easy to obtain, making it suitable for further utilization.

In this study, ZnAl LDH was converted into 3 other derivative materials. ZnAl LDH is calcined into ZnAl LDO and composited with GME to obtain ZnAl LDH-GME and ZnAl LDO-GME. The characteristics of the four synthesized catalysts were studied using XRD, FT-IR, UV-DRS, and SEM EDX. The performance of the photocatalyst was determined through the degradation of TC under solar light irradiation. Degradation kinetics were also ascertained, along with changes in catalyst mass, pH, and contact time. The ZnAl LDH-based derivative materials structure's stability was evaluated using catalyst regeneration for a total of five cycles.

2. EXPERIMENTAL SECTION

2.1 Instrumentals dan Chemicals

XRD Rigaku MiniFlex 600, FT-IR Alpha BRUKER Spectrophotometer, Jasco V-760 UV-DRS (200-800 nm), and Scanning Electron Miscroscope-EDX Zeiss/SEM EVO MA 10 were all employed in this investigation. At a wavelength of 354 nm, the Shimadzu UV-1900 UV-Vis Spectrophotometer was used to analyze TC degradation.

For the generation of M^{2+} and M^{3+}, $Zn(NO_3)_2.6H_2O$ (Merck) and $Al(NO_3)_3.9H_2O$ (Merck) are the materials employed. The Merck supplied NaOH. The source of 96% technical ethanol and distilled water was PT Bratachem Indonesia. Indonesian Mangosteen pericarp (*Garcinia mangostana*) was collected at Palembang, South Sumatra. The TC waste was generated from Tetracycline HCl tablets of 500 mg purchased from Holi Pharma Indonesia.

2.2 Mangosteen (*Garcinia mangostana*) Pericarp Extraction

The dried mangosteen (*Garcinia mangostana*) pericarp was crus hed and extracted with 96% technical ethanol. A maceration method proposed by Ghuzali et al. (2021) is used in the GM extraction process. GM powder was saturated 1:10 in 96% technical ethanol for 3×24 hours. Rotary Vacuum Evaporators concentrate GM powder extract to generate GM extract (GME). FT-IR characterized the GME.

2.3 ZnAl LDH-Based Composite Preparation

The ZnAl-LDH catalyst was prepared using the coprecipitation method, as described by Lesbani et al. (2020). A total of 100 mL each of $Zn(NO_3)_2.6H_2O$ and $Al(NO_3)_3.9H_2O$ solutions with a ratio of 3:1 was mixed in a glass beaker. While the solution was homogenized with magnetic stirring, 2 M NaOH was added until the pH was 8. The stirring procedure was maintained at 70°C for four hours. The filtered precipitate was washed using distilled water and oven-dried at 100°C. The final product was ZnAl-LDH. By calcining ZnAl-LDH for four hours at 500°C, ZnAl-LDO was obtained.

The restacking procedure by Muráth et al. (2023) was modified to generate ZnAl LDH/LDO composites with GME. In a 50 mL aquadest, each 3 g of ZnAl LDH/LDO was sonicated

for 20 minutes. After that, 3 grams of GME were added to each solution containing ZnAl LDH and ZnAl LDO under a nitrogen atmosphere. Afterwards, the mixture was stirred using a magnetic stirrer at a temperature of 80°C for 24 hours. The resulting precipitate was dried at 60°C in an oven after cleaning with 90% ethanol. The dry precipitates obtained were ZnAl LDH-GME and ZnAl LDO-GME catalysts. The four materials obtained in this method were analyzed using XRD, FT-IR, UV-DRS, and SEM-EDX.

2.4 Studies of Photodegradation Activity

Four prepared ZnAl LDH-based composites are used in a batch system as catalysts in the photodegradation of TC. A beaker holding 20 mL of 5 mg/L TC was mixed with the catalysts. The solution was shaken at 250 rpm under solar light irradiation from 11.00 until 13.00 (10000 lux). The optimal catalyst mass was determined by varying catalyst mass. The influence of pH was investigated by varying the TC solution pH to 3, 5, 7, 9, and 11. The degradation kinetics have been calculated by studying the result of exposure duration.

2.5 Catalyst Regeneration

The catalyst's regeneration activity is demonstrated by its capacity to be used iteratively (Ahmad et al., 2023b). Used catalysts were ultrasonically cleaned for 30 minutes in 50 mL of distilled water. Following the previous procedure, the dry and clean catalyst was used up to five times for the degradation of tetracycline. The regeneration percentage is calculated using Equation 1.

$$\%R = \left(\frac{C_0 - C_t}{C_0}\right) \times 100 \quad (1)$$

3. RESULTS AND DISCUSSIONS

3.1 ZnAl LDH-Based Composite Characterization

Figure 1 depicts the characteristics of the functional groups contained in the generated catalysts. A typical LDH-based material spectra is shown by ZnAl LDH. The existence of −OH vibrations in the metal layer can be verified by the peak at 3400 cm^{-1}. Wave numbers 1600 cm^{-1} and 1300 cm^{-1} correspond to interlayer water molecules and NO3- vibrations. Typical vibrations of ZnO and AlO metal oxides are seen at the peak at 500–800 cm^{-1} (Ahmad et al., 2023b; Hanifah et al., 2023b; Hanifah et al., 2023a). The calcination method eliminates water molecules and −OH groups from ZnAl LDH, eliminating −OH vibrations (3390 cm^{-1}) in ZnAl LDO.

The composite spectra of ZnAl LDH-GME and ZnAl LDO-GME demonstrate composite precursor materials. Palapa and Wijaya (2023) reported that the combined FT-IR spectra of precursor materials in composite materials may indicate the success of the composite synthesis process. GME's characteristic vibration peaks at 2800-2900 cm^{-1} and 1500-1600 cm^{-1} reflect asymmetric stretching of the methylene group (CH_2) and C=C stretching of the aromatic ring (Yasir et al., 2022). The new absorptions at 1441 cm^{-1}, 1271 cm^{-1}, and 1000-1200 cm^{-1} indicate CH_2 bending vibrations, C−O stretching, and C−OH stretching vibrations (Aminah et al., 2014; Rahayua and Yamtinaha, 2018; Yasir et al., 2022). The presence of many GME-typical active groups in ZnAl LDH and ZnAl LDO suggests that the ZnAl LDH-GME and ZnAl LDO-GME composites were synthesised effectively.

Figure 2 depicts the X-Ray diffraction pattern of the prepared catalysts. ZnAl LDH diffractogram is consistent with standard JCPDS 38-0486, exhibiting peaks at 2θ = 10-11° (003), 20.17° (006), 29.54° (112), 31.92° (104), 34.43° (015), 36.31° (107), 60.47° (110), and 61.34° (113) (Ahmad et al., 2023). Peaks at 2θ angles of 10-11° and 60-62° suggest a layered structure of LDH, with metal cations dispersed (Ahmad et al., 2023b; Hanifah et al., 2023b; Hanifah et al., 2023a). The ZnAl LDO diffraction pattern is consistent with JCPDS 36-1451. However, the peak at 2θ = 10–11° disappears due to calcination destroying the layered structure of LDH (Gao et al., 2019; Lesbani et al., 2020; Wang et al., 2021). The diffractogram of ZnAl LDH-GME differs from pristine LDH. The LDH peak remains detectable in ZnAl LDH-GME but not at 2θ 30°-40° angle range. The comparable peaks at an angle of 2θ between ZnAl LDO and ZnAl LDO-GME indicate that ZnAl LDO-GME is equally at the site of composite generation by coating. The coating on the ZnAl LDH/LDO by GME bioactive chemicals hides the ZnAl LDH/LDO crystal structure, decreasing crystallinity and causing a sloper diffraction peak (Ahmad et al., 2023a). The XRD diffraction pattern further proves the successful synthesis of ZnAl LDH-GME and ZnAl LDO-GME composites.

The light absorption capacity of the constructed catalysts was investigated using UV-DRS (Figure 3). ZnAl LDH-GME and ZnAl LDO-GME composites exhibit UV and visible light absorption capabilities. Unlike its precursors, ZnAl LDH and ZnAl LDO exclusively absorb UV light. The bandgap energy may be obtained by the Tauc Plot in UV-DRS analysis (Jubu et al., 2022). The band gap energy of ZnAl LDH and ZnAl LDO coated by GME reduces from 3.56 to 2.33 eV and 3.10 to 2.93 eV, respectively. ZnAl LDH-GME and LDO-GME composites with carbon-rich GME and conjugated bonds have enhanced charge separation and hole lifespan, reducing electron recombination and enhancing degradation (Katwal et al., 2021; Cong et al., 2023). In the photodegradation system, modified ZnAl absorbs photons from various light, generating more O_2^- and OH radicals and enhancing photocatalytic activity (Otgonbayar and Oh, 2023).

The synthesized catalysts' surface shape is displayed in the 10,000-times magnification SEM image (Figure 4). The surfaces of ZnAl LDH/LDO are irregular. A catalyst with a more evenly distributed surface is generated when GME is added. The surface of ZnAl LDH-GME has a morphology characterized by thin wrinkles, while ZnAl LDO-GME displays equally scattered little grains. The dispersion of the elements in the ZnAl composite coated with GME is shown in the element

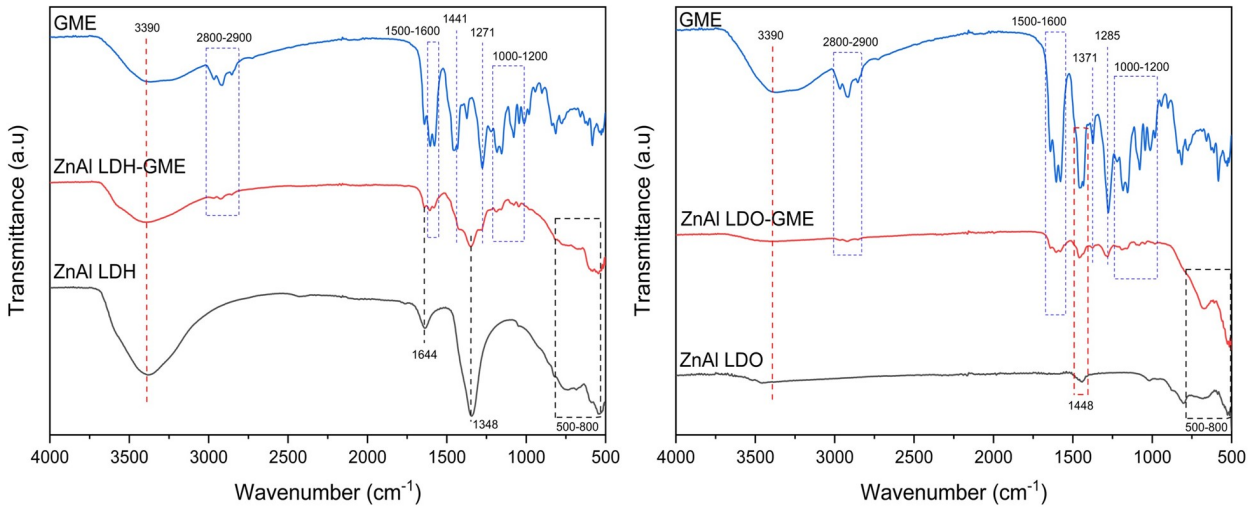

Figure 1. The Prepared Catalysts' FT-IR Spectra

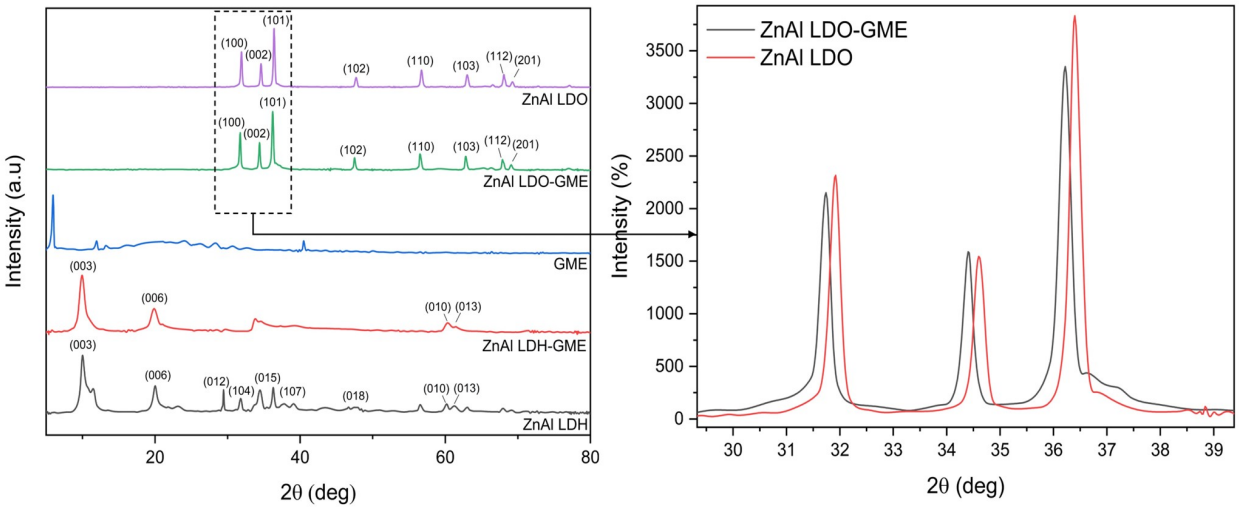

Figure 2. The Synthsized Catalysts' XRD Pattern

distribution mapping of the ZnAl LDH-GME and ZnAl LDO-GME catalysts (Figure 4(e) and (f)). The surface of ZnAl LDH-GME is mainly composed of carbon (C) derived from GME. This suggests that GME creates a composite by covering the ZnAl LDH's surface. In contrast to ZnAl LDO-GME, element mapping reveals the existence of C in the bottom layer of Zn and Al. GME may intercalate the ZnAl LDO interlayer. A combination of bioactive chemicals from GME stretches the ZnAl LDO layer into a monolayer. XRD results verify this since the ZnAl LDO-GME diffractogram does not display typical layered structure of LDH material.

Adding GME altered the material particle size (Figure 5). Previous investigations have verified that secondary metabolites include bioactive chemicals that may function as chelating (Ezhilarasi et al., 2018; Cong et al., 2023). Due to electron charge stabilization, GME binding to the catalyst surface breaks ZnAl bonds. Consequently, ZnAl LDH-GME and ZnAl LDO-GME exhibit a surface morphology with reduced particle sizes compared to their precursor materials. This process is further complicated by changes in the atomic composition of the catalyst (see Table 1). Due to its carbon-rich nature, GME boosts the carbon (C) proportion in the ZnAl LDH-GME catalyst from 2.02% to 44.44% and in the LDO-GME catalyst from 8.13% to 36.85%. This confirms that the formation of composites by adding GME successfully generated ZnAl LDH-GME and ZnAl LDO-GME.

3.2 Catalyst Mass Optimization

Figure 6(a) depicts the results of the catalysts' mass optimization. The optimal degradation performance of ZnAl LDH, LDO, and LDH-GME was 20 mg, whereas ZnAl LDO-GME

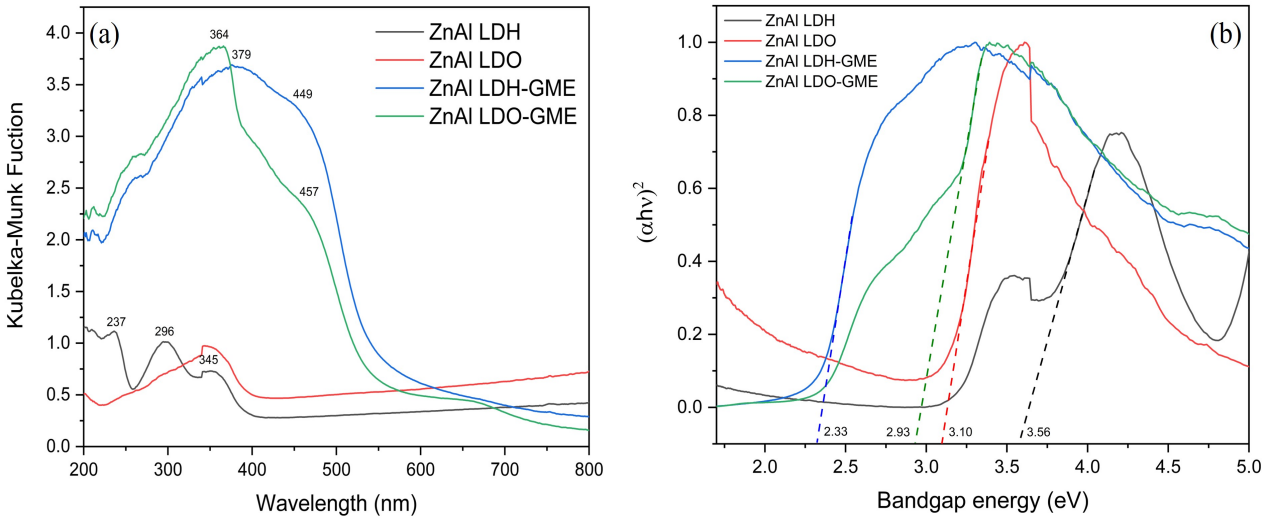

Figure 3. Light Response (a); and Bandgap Energy (b) of the Synthesized Catalysts

was 5 mg, respectively, 63.32%, 97.75%, 83.28%, and 56.62%. More active sites are present on the surface of ZnAl LDO-GME, as shown by its optimal photodegradation performance at a lesser mass when compared to the other three catalysts. Performance of degradation is decreased by adding mass of ZnAl LDO-GME. An excessive quantity of catalyst obscures the solution and inhibits light access. Thus, ZnAl LDO-GME absorbs less light and produces fewer holes (Devi et al., 2023; Oladipo, 2021). The other three catalysts degraded more efficiently as catalytic mass increased, unlike ZnAl LDO-GME. Enhancing the mass of the catalyst leads to an increased quantity of active sites that may absorb photons and generate reactive radicals (Tajat et al., 2024). Considering this, the catalyst's mass affects photodegradation.

3.3 pH Optimization

Figure 6(b) demonstrates how pH affects synthesized catalysts in TC photodegradation. Photodegradation is affected by pH (Ahmad et al., 2023b; Des, 2022; Kah et al., 2007). Alterations in pH will affect both the catalysts' surface charge ang the TC molecule structure (Li et al., 2023a; Song et al., 2022). This research investigated the impact of pH by varying the pH levels of the sample solution to 3, 5, 7, 9, and 11, using 0.1 M HCl and 0.1 M NaOH as additions. At pH 5, ZnAl LDH, ZnAl LDO, ZnAl LDH-GME, and ZnAl LDO-GME exhibited the highest percentage of TC degradation (63.32%, 97.75%, 83.28%, and 56.62% at the 90-minute mark, respectively). Boukhalfa et al. (2017) and Zahara et al. (2023) have shown that ZnAl LDH has a pHpzc range of 6-8. Within this pH range, the catalyst surface is inclined towards neutrality and demonstrates optimal photocatalytic activity (Ahmad et al., 2023b). The ZnAl LDO, lacking the −OH group, exhibits less protonation at pH 5, allowing it to maintain a neutral charge at this pH (Ariza-Tarazona et al., 2020).

TC structure is also affected by pH. The pH variations lead to changes in the concentration of TC in the solution. The TC solution has a natural pH of 5, allowing it to exist in its neutral molecular state, making it susceptible to degradation. Excess free H^+ at pH below 5 inhibits the active generation of free radicals and electron-hole pair separation, resulting in limited degradation (Li et al., 2023d). On the other hand, the catalyst might become ineffective in an alkaline condition. This may occur when excess hydroxide ions (OH^-) in the solution combine with OH radicals generated by the catalyst. Consequently, the hydroxyl radicals will be deactivated, reducing the photocatalytic activity (Li et al., 2023b; Song et al., 2022).

3.4 Photodegradation of TC

The photodegradation was performed in optimal conditions for each catalyst, with a 20 mL solution containing 5 mg/L of TC. The photodegradation occurs under solar light (10,000 lux at 11 a.m.–1 p.m.), with the first 30 minutes of adsorption. With photocatalytic activity up to 97.75% of TC degradation in 90 minutes, ZnAl LDO is the most effective catalyst (see Figure 7a). Calcinating ZnAl LDH to LDO generated a metal oxide-like catalyst without interlayer anion and shorter interlayer distances (Mo et al., 2023). This material structure allowed ZnAl LDO to remove TC from the solution through 2 simultaneous mechanisms: adsorption and degradation (Rohmatullaili et al., 2024). The interlayer space without anions in ZnAl LDO could act as the adsorption site for TC, while some other TC was degraded in the outer metal layer of ZnAl LDO. As a result, ZnAl LDO showed the best catalytic performance compared to other catalysts in this study.

LDH-based material holds sufficient flexibility to allow for the degradation on its outer surface while simultaneously repairing the interlayer via adsorption (Rohmatullaili et al., 2024). Investigations showed that specific materials may act as both adsorbents and catalysts (Desgagnés and Iliuta, 2023; Pan et al., 2023; Wang et al., 2023b). Unlike ZnAl LDO-GME, the in-

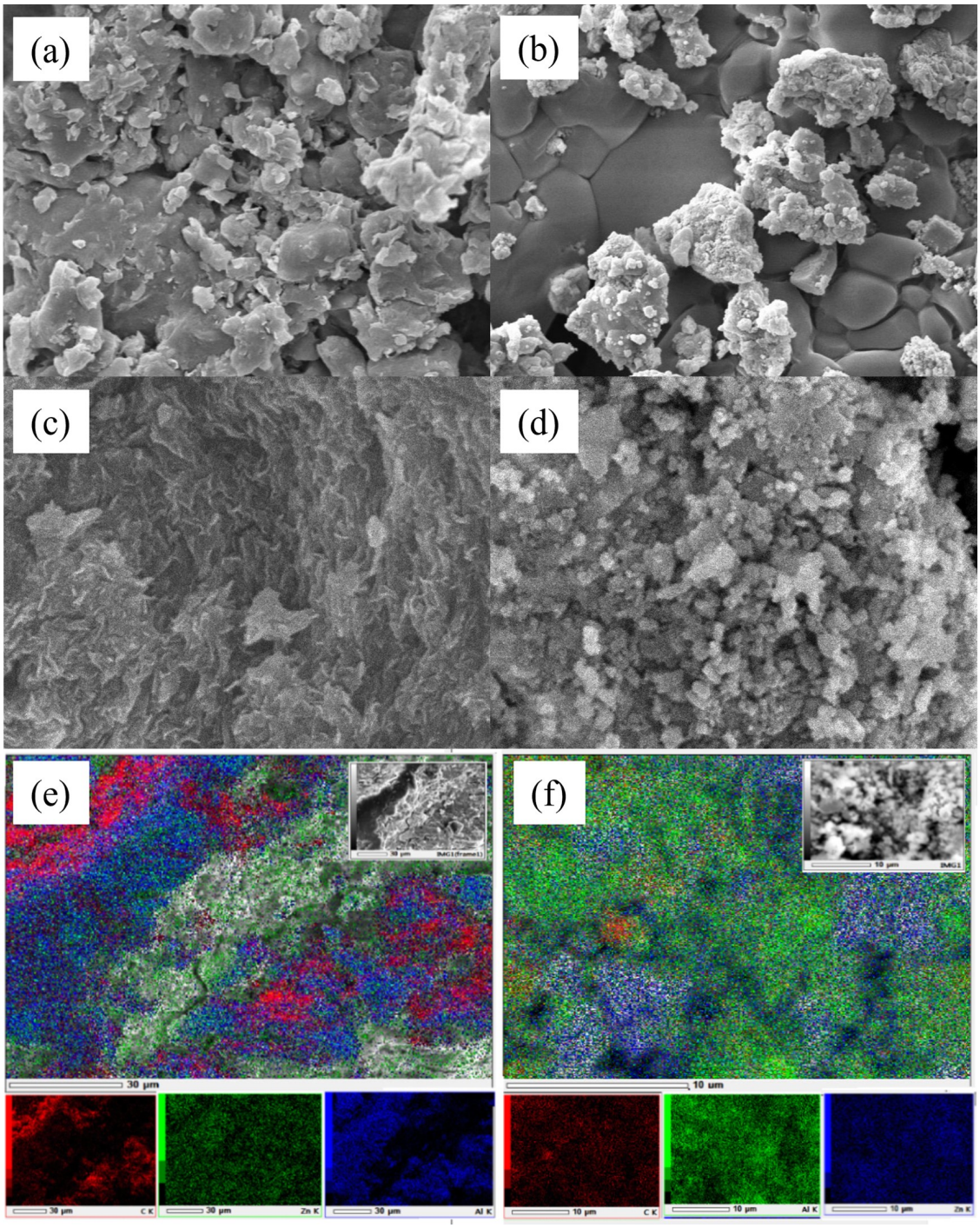

Figure 4. SEM Image of ZnAl LDH (a), ZnAl LDO (b), ZnAl LDH-GME (c), and ZnAl LDO-GME (d); Element Mapping of ZnAl LDH-GME (e), and ZnAl LDO-GME (f)

tercalation of GME on ZnAl LDO results in the interlayer distance increasing until it approaches the level of a single layer. As a consequence, there are fewer active sites than ZnAl LDO, and degradation efficiency is just 56.62%.

ZnAl LDH degraded 63.32% TC. The massive number of active sites that ZnAl LDH provides as an LDH-based material is one of its advantages (Silaen et al., 2021). However, photodegradation is also impacted by the light source. Figure 3a demonstrates that ZnAl LDH exhibits poor responsiveness to visible light. Hence, the utilization of solar light fails to induce the optimum performance of ZnAl LDH as a photocatalyst. The incorporation of GME to ZnAl LDH formed ZnAl

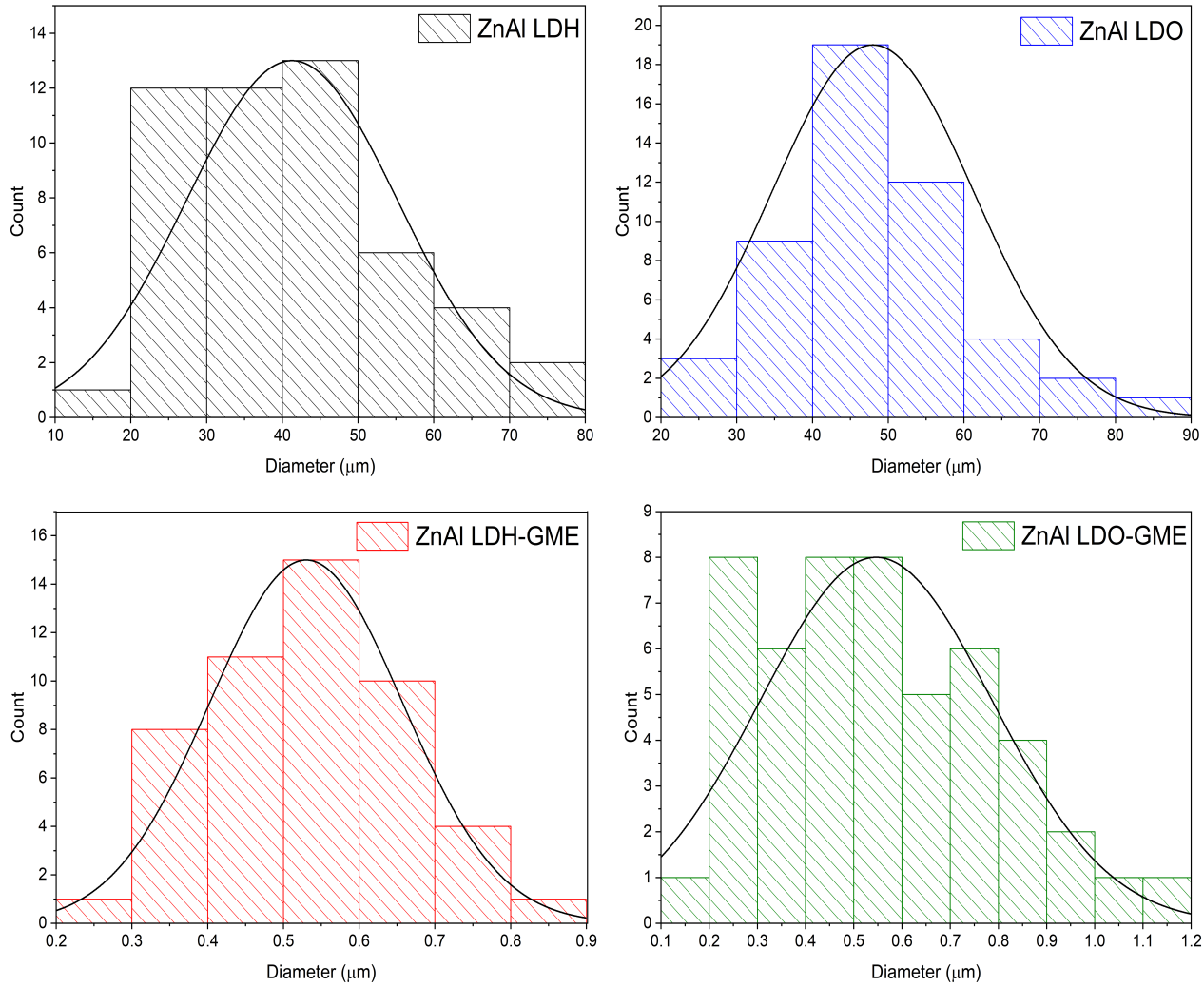

Figure 5. Catalysts' Particle Size Distribution

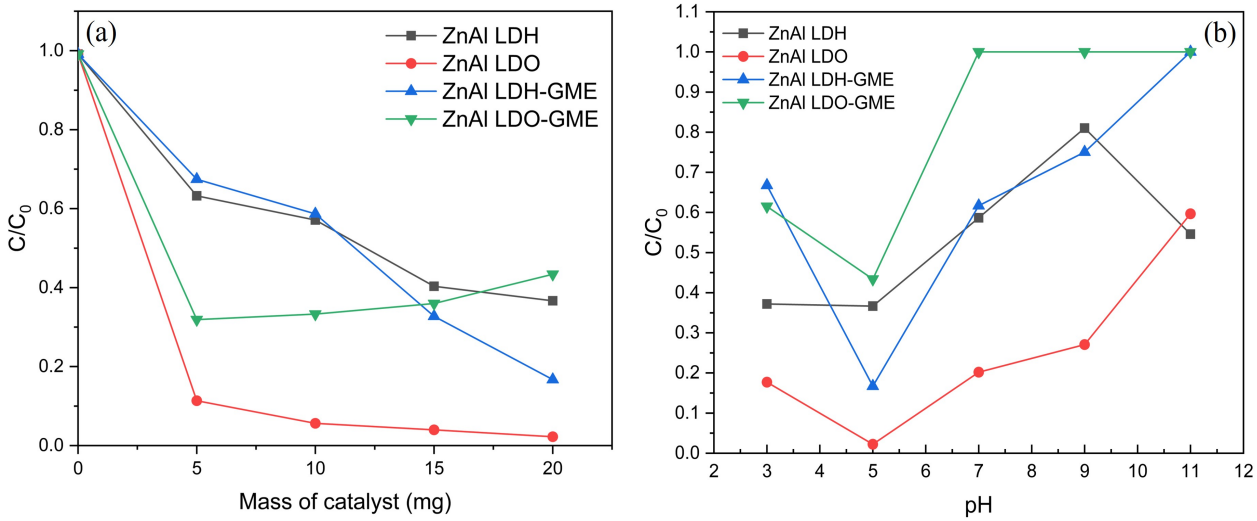

Figure 6. Effect of Catalyst' Mass (a); and Effect of pH (b)

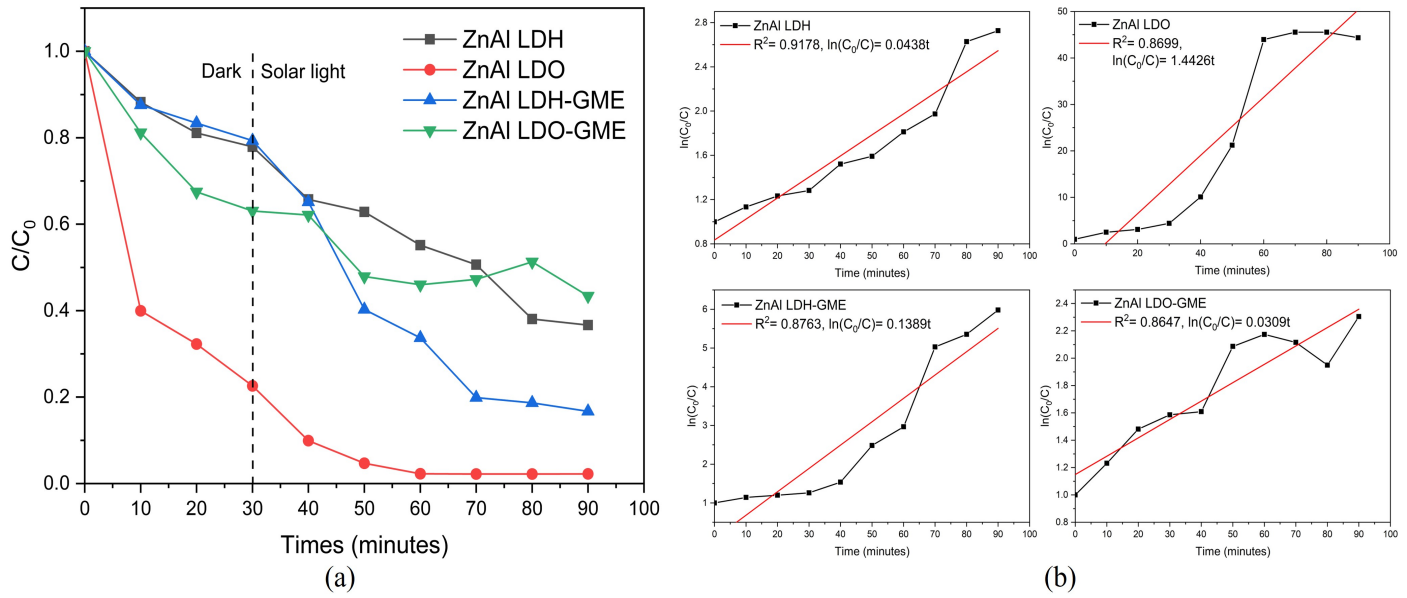

Figure 7. Effect of Photodegradation Time (a); Kinetics of TC Photodegradation (b)

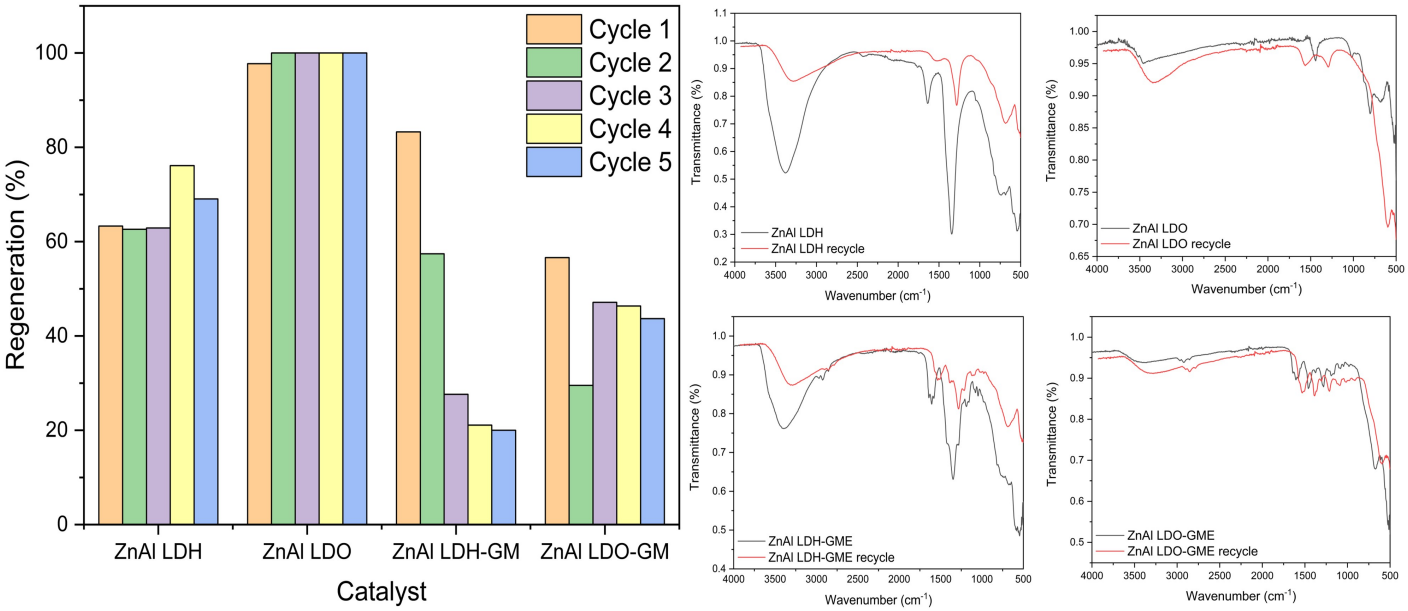

Figure 8. Regeneration of Catalysts (a); and FT-IR Spectra Comparison of Fresh and Recycle Catalyst (b)

LDH-GME, adjusting the catalyst's response to solar light and improving its catalytic activity to 83.28%. The catalytic performance comparison of the synthesized catalysts in this study to several catalysts for TC degradation is shown in Table 2.

TC degradation kinetics were examined in min^{-1} using the integral of the mitigated Langmuir-Hinshelwood (LH) equation. Kinetic parameters were determined by plotting ln(C0/C) toward time (Yuliasari et al., 2022). Formula findings are shown in Figure 7b. The four catalysts degraded TC at the same rate as efficiently. The ZnAl LDO catalyst had the most significant deterioration rate compared to all other catalysts (1.4426 min^{-1}), while the ZnAl LDO-GME catalyst had the lowest degradation rate among all catalysts (0.0309 min^{-1}). Adding GME to ZnAl LDH to create a composite increased degradation by three times, reaching 0.1389 min^{-1} from 0.0438 min^{-1}.

3.5 Regeneration of Catalysts

The catalyst's reusability is shown by its percent regeneration (Figure 8a). ZnAl LDO has the highest efficiency among cata-

Table 1. Atom Percentage of Catalysts

Atom	% Atom of			
	ZnAl LDH	ZnAl LDH-GME	ZnAl LDO	ZnAl LDO-GME
Zn	6.78	6.68	15.18	13.92
Al	0.62	2.77	2.57	6.77
C	2.02	44.44	8.13	36.85
N	3.19	9.46	15.71	6.04
O	28.19	36.64	58.09	36.43
H	59.2	0	0.32	0

Table 2. The Photocatalytic Performance of Various Catalysts in TC Degradation

Catalysts	Degradation (%)	Irradiation time	Reference
In_2S_3/Zn–Al LDH Composite (1:4)	77.00	30	(Wang et al., 2022a)
ZnCr-LDH	59.00	90	(Zhu et al., 2023)
MgAl LDH	59.70	105	(Sun et al., 2022)
Ag_2O-Ag/ZnAl-LDO	80.00	90	(Shen et al., 2020)
NiAl LDH/$Ag_6Si_2O_7$	58.50	120	(Xu et al., 2023a)
NiFe LDH	67.20	90	(Zheng et al., 2020)
NiAl LDH/ $Bi_{28}O_{32}(SO_4)_{10}$	95.00	120	(Li et al., 2023a)
CuCo-LDO/CN (1:5)	48.00	40	(Gu et al., 2023)
ZnAl LDH-CT	66.37	90	(Rohmatullaili et al., 2024)
ZnAl LDO-CT	56.05	90	(Rohmatullaili et al., 2024)
ZnAl LDH	63.32	90	This study
ZnAl LDO	97.75	90	This study
ZnAl LDH-GME	83.28	90	This study
ZnAl LDO-GME	56.62	90	This study

lysts. The use of ZnAl LDH and LDO in the fifth regeneration cycle resulted in a higher regeneration percentage compared to the first use. The regeneration process may induce this effect as a result of ultrasonic treatment. According to Li et al. (2023c) and Ye et al. (2022), ultrasonic treatment might form nanosheets by stretching metal layers and dispersing the primary metal layer. Numerous studies revealed that the capacity to transform LDH into LDH nanosheets by ultrasonic treatment is one of the unique characteristics of LDH-based materials (Hao et al., 2024; Kameda et al., 2021). The ZnAl LDH regeneration enhanced the active site openness. Meanwhile, repeated use of ZnAl LDO resulted in the addition of OH groups as active sites in the degradation process. This was further confirmed through functional group analysis using FT-IR.

The FT-IR investigation of the fifth cycle of ZnAl LDO (as seen in Figure 8b) reveals an enhancement in the presence of −OH groups and water molecules inside the interlayer. This suggests that water molecules intercalate with recurrent degradation. ZnAl LDO degraded 100% of TC after attaching the −OH group in the second cycle. Due to its similarities to metal oxides, ZnAl LDO molecular structure is stable without altering functional groups. The mixed metal oxide layer's structural stability was proven to be outstanding when exposed to repeated use (Momin et al., 2023).

FT-IR spectrum in Figure 8b shows that ZnAl LDH and ZnAl LDH-GME have fewer active sites and regenerate less due to −OH group reduction. These findings indicate that both ZnAl LDH and ZnAl LDH-GME exhibit less stable structures. After five times ultrasonically cleaning, ZnAl LDH-GME and LDO-GME may be mashed and reduced. Repeated cycles of ZnAl LDH-GME and LDO-GME distort the TC solution and limit light penetration. This lowers the regeneration percentage for each cycle. Nevertheless, the repeated use of ZnAl LDO-GME did not induce any alterations to the composition of the ZnAl LDO-GME. ZnAl LDO-GME structure stability is increased by aromatic groups from GME surrounding the primary metal layer (Muráth et al., 2023; Siregar et al., 2021).

4. CONCLUSIONS

The combination of coprecipitation, calcination, and restacking procedures successfully synthesized and modified ZnAl LDH-based material. Calcinating ZnAl LDH at 500°C produced ZnAl LDO, which loses its layered structure and resembles a metal oxide mixture. Composites of ZnAl LDH/LDO-GME were successfully generated by adding GME to ZnAl LDH

and LDO, confirmed by XRD, FT-IR, and SEM-EDX spectra. UV-DRS study shows that the catalyst without GME only reacts to UV light, whereas the GME composite responds to visible light. The presence of GME breaks ZnAl molecular bonds, reducing particle size. ZnAl LDO experienced the most excellent effectiveness in degrading TC under solar light irradiation, with a removal rate of up to 97.75% during a 90-minute timescale. Furthermore, ZnAl LDO has excellent structural stability after five usage cycles; in the fifth regeneration cycle, ZnAl LDO may even completely eliminate TC.

5. ACKNOWLEDGMENT

The authors express their gratitude to the Research Center of Inorganic Materials and Complexes at Universitas Sriwijaya for providing the required chemicals, laboratory equipment, and characterization services. The authors also acknowledge the UIN Raden Fatah Palembang Integrated Laboratory for instrumental analysis.

REFERENCES

Abed, M. F. and A. A. Faisal (2023). Calcium/Iron-Layered Double Hydroxides-Sodium Alginate for Removal of Tetracycline Antibiotic from Aqueous Solution. *Alexandria Engineering Journal*, **63**; 127–142

Ahmad, N., F. S. Arsyad, I. Royani, and A. Lesbani (2023a). Charcoal Activated As Template Mg/Al Layered Double Hydroxide for Selective Adsorption of Direct Yellow on Anionic Dyes. *Results in Chemistry*, **5**; 100766

Ahmad, N., F. S. Arsyad, I. Royani, P. M. S. B. N. Siregar, T. Taher, and A. Lesbani (2023b). High Regeneration of ZnAl/NiAl-Magnetite Humic Acid for Adsorption of Congo Red from Aqueous Solution. *Inorganic Chemistry Communications*, **150**; 110517

Ahmed, M. A., M. A. Ahmed, and A. A. Mohamed (2023). Adsorptive Removal of Tetracycline Antibiotic onto Magnetic Graphene Oxide Nanocomposite Modified with Polyvinylpyrroilidone. *Reactive and Functional Polymers*, **191**; 105701

Ajiboye, T. O., L. Saunyama, M. Ravele, A. A. Rasheed-Adeleke, N. Seheri, D. C. Onwudiwe, and S. D. Mhlanga (2023). Synthesis Approaches to Ceramic Membranes, Their Composites, and Application in the Removal of Tetracycline from Water. *Environmental Advances*, **12**; 100371

Aladpoosh, R. and M. Montazer (2022). Functionalization of Cellulose Fibers Alongside Growth of 2D LDH Platelets through Urea Hydrolysis Inspired Taro Wettability. *Carbohydrate Polymers*, **275**; 118584

Aminah, L. N., S. Leong, C. Ho, Y. Wong, and C. Kairulazam (2014). Characterization of *Garcinia mangostana Linn.* Seeds As Potential Feedstocks for Biodiesel Production. *International Journal of Engineering and Technology*, **6**(2); 146

Angasa, E., Y. E. Putri, N. Jamarun, and S. Arief (2020). Improving the Morphological, Optical, and Photocatalytic Properties of Octahedral Zn_2SNO_4 Using *Garcinia mangostana* Fruit Peel Extract. *Vacuum*, **182**; 109719

Ariza-Tarazona, M. C., J. F. Villarreal-Chiu, J. M. Hernández-López, J. R. De la Rosa, V. Barbieri, C. Siligardi, and E. I. Cedillo-González (2020). Microplastic Pollution Reduction by a Carbon and Nitrogen-Doped TiO_2: Effect of pH and Temperature in the Photocatalytic Degradation Process. *Journal of Hazardous Materials*, **395**; 122632

Asadpour, S., N. Sarmast, Z. Aramesh-Boroujeni, and N. Sadegh (2023). Enhanced Adsorption Performance of Tetracycline in Aqueous Solutions Using Mg-Al-LDH/AC Nanocomposite. *Arabian Journal of Chemistry*, **16**(12); 105301

Azalok, K. A., A. A. Oladipo, and M. Gazi (2021). Hybrid MnFe-LDO–Biochar Nanopowders for Degradation of Metronidazole Via UV-Light-Driven Photocatalysis: Characterization and Mechanism Studies. *Chemosphere*, **268**; 128844

Boukhalfa, N., M. Boutahala, and N. Djebri (2017). Synthesis and Characterization of ZnAl-Layered Double Hydroxide and Organo-K10 Montmorillonite for the Removal of Diclofenac from Aqueous Solution. *Adsorption Science & Technology*, **35**(1-2); 20–36

Cong, C. Q., N. M. Dat, N. D. Hai, N. T. H. Nam, H. An, T. Do Dat, N. T. Dat, M. T. Phong, and N. H. Hieu (2023). Green Synthesis of Carbon-Doped Zinc Oxide Using *Garcinia mangostana* Peel Extract: Characterization, Photocatalytic Degradation, and Hydrogen Peroxide Production. *Journal of Cleaner Production*, **392**; 136269

Des, K. (2022). Factors Affecting Microbial Degradation. *Global Science Research Journals*, **10**(2); 1–2

Desgagnés, A. and M. C. Iliuta (2023). Intensification of CO_2 Hydrogenation by In-Situ Water Removal Using Hybrid Catalyst-Adsorbent Materials: Effect of Preparation Method and Operating Conditions on the RWGS Reaction As a Case Study. *Chemical Engineering Journal*, **454**; 140214

Devi, S. K., V. Thirumal, A. Balamurugan, B. Avula, U. D. Pongiya, J. Kim, and C. Surya (2023). Photocatalytic Degradation of Tetracycline Over Ternary NiCOMn-LDH under Visible Light Illumination. *Materials Letters*, **350**; 134910

Ezhilarasi, A. A., J. J. Vijaya, K. Kaviyarasu, L. J. Kennedy, R. J. Ramalingam, and H. A. Al-Lohedan (2018). Green Synthesis of NiO Nanoparticles Using Aegle Marmelos Leaf Extract for the Evaluation of In-Vitro Cytotoxicity, Antibacterial and Photocatalytic Properties. *Journal of Photochemistry and Photobiology B: Biology*, **180**; 39–50

Faisal, S., H. Jan, S. A. Shah, S. Shah, A. Khan, M. T. Akbar, M. Rizwan, F. Jan, Wajidullah, and N. Akhtar (2021). Green Synthesis of Zinc Oxide (ZnO) Nanoparticles Using Aqueous Fruit Extracts of Myristica Fragrans: Their Characterizations and Biological and Environmental Applications. *ACS Omega*, **6**(14); 9709–9722

Gao, B., J. Zhou, H. Wang, G. Zhang, J. He, Q. Xu, N. Li, D. Chen, H. Li, and J. Lu (2019). Zeolitic Imidazolate Framework 8-Derived Au@ ZnO for Efficient and Robust

Photocatalytic Degradation of Tetracycline. *Chinese Journal of Chemistry*, **37**(2); 148–154

Gholami, P., A. Heidari, A. Khataee, and M. Ritala (2023). Oxygen and Nitrogen Plasma Modifications of ZnCuCO LDH-Graphene Nanocomposites for Photocatalytic Hydrogen Production and Antibiotic Degradation. *Separation and Purification Technology*, **325**; 124706

Gholami, P., A. Khataee, R. D. C. Soltani, L. Dinpazhoh, and A. Bhatnagar (2020). Photocatalytic Degradation of Gemifloxacin Antibiotic Using Zn-CO-LDH@ Biochar Nanocomposite. *Journal of Hazardous Materials*, **382**; 121070

Ghuzali, N. A. M., M. A. A. C. M. Noor, F. A. Zakaria, T. S. Hamidon, and M. H. Husin (2021). Study on *Clitoria ternatea* Extracts Doped Sol-Gel Coatings for the Corrosion Mitigation of Mild Steel. *Applied Surface Science Advances*, **6**; 100177

Gu, Y.-Y., Z. Wu, Y. Shen, C. Lu, L. Lu, Z. Bian, X. Zhang, C. Zhao, R. Fu, and H. Li (2023). Efficient Fenton-Like Degradation of Tetracycline by Stalactite-Like CuCO-LDO/CN Catalysts: The Overlooked Contribution of Dissolved Oxygen. *Chemosphere*, **338**; 139540

Hanifah, Y., R. Mohadi, and A. Lesbani (2023a). Photocatalytic Degradation of Rhodamine-B by Ni/Zn LDH Intercalated Polyoxometalate Compound. *Science and Technology Indonesia*, **8**(1); 93–99

Hanifah, Y., R. Mohadi, and A. Lesbani (2023b). Polyoxometalate Intercalated MgAl-Layered Double Hydroxide for Degradation of Malachite Green. *Ecological Engineering & Environmental Technology*, **24**(2); 109–119

Hao, T., H. Xu, S. Sun, H. Yu, Q. Qin, B. Song, M. Li, G. Shao, B. Fan, and H. Wang (2024). Assembling Flower-Like MgAl-LDH Nanospheres and g-C_3N_4 Nanosheets for High Efficiency Removal of Methyl Orange. *Ceramics International*, **50**(7); 10724–10734

Isnaeni, I. N., D. Sumiarsa, and I. Primadona (2021). Green Synthesis of Different TiO_2 Nanoparticle Phases Using Mango-Peel Extract. *Materials Letters*, **294**; 129792

Jubu, P. R., O. Obaseki, A. Nathan-Abutu, F. Yam, Y. Yusof, and M. Ochang (2022). Dispensability of the Conventional Tauc's Plot for Accurate Bandgap Determination from UV–Vis Optical Diffuse Reflectance Data. *Results in Optics*, **9**; 100273

Kah, M., S. Beulke, and C. D. Brown (2007). Factors Influencing Degradation of Pesticides in Soil. *Journal of Agricultural and Food Chemistry*, **55**(11); 4487–4492

Kameda, T., K. Horikoshi, H. Kikuchi, F. Kitagawa, S. Kumagai, Y. Saito, M. Kondo, Y. Jimbo, and T. Yoshioka (2021). Kinetic and Equilibrium Analyses of Lactate Adsorption by Cu-Al and Mg-Al Layered Double Hydroxides (Cu-Al LDH and Mg-Al LDH) and Cu-Al and Mg-Al Layered Double Oxides (Cu-Al LDO and Mg-Al LDO). *Nano-Structures & Nano-Objects*, **25**; 100656

Katwal, R., R. Kothari, and D. Pathania (2021). *An Overview on Degradation Kinetics of Organic Dyes by Photocatalysis Using Nanostructured Electrocatalyst*. Elsevier

Lee, D.-E., M. Danish, and W.-K. Jo (2024). Two in One is Really Better: NiAl-LDH/[CoNi (μ3-tp) 2 (μ2-py)2] Nanocomposite for Enhanced Antibiotic Norfloxacin Degradation and H_2 Evolution Reaction. *Separation and Purification Technology*, **332**; 125748

Lesbani, A., T. Taher, N. R. Palapa, R. Mohadi, A. Rachmat, and Mardiyanto (2020). Preparation and Utilization of Keggin-Type Polyoxometalate Intercalated Ni–Fe Layered Double Hydroxides for Enhanced Adsorptive Removal of Cationic Dye. *SN Applied Sciences*, **2**(3); 1–4

Li, H., Z. Zhu, C. Hu, J. Zheng, and B. Liu (2023a). Preparation of S-Scheme Heterojunction $Bi_{28}O_{32}$ (SO_4) 10/NiAl LDH for Efficient Photocatalytic Degradation of Tetracycline. *Advanced Powder Technology*, **34**(7); 104066

Li, J., H. Cao, H. Qi, Y. Li, S. Zhu, X. Ye, J. Zhang, Z. Yu, J. Zhu, and X. Zhao (2023b). Efficiently Activating Peroxymonosulfate by CoFe-LDHs/MoS_2 for Rapid Degradation of Tetracycline. *Journal of Water Process Engineering*, **53**; 103856

Li, Q., H. Cao, F.-F. Chen, and Y. Yu (2023c). Boosting Charge Transfer of NiAl-LDH by Silicate Nanosheets for Enhanced Photocatalytic CO_2 Reduction. *Materials Letters*, **351**; 135101

Li, Z., H. Li, X. Zeng, S. Liu, and Y. Yang (2023d). Adsorption and Photodegradation of Tetracycline by Mannose-Grafted Chitosan Composite Films: Performance, Mechanism and Availability. *Chemical Engineering Journal*, **458**; 141455

Mo, W., Y. Yang, C. He, Y. Huang, and J. Feng (2023). Excellent Adsorption Properties of Mg/Al/Fe LDOs for Cr (VI) in Water. *Journal of Environmental Chemical Engineering*, **11**(5); 111069

Momin, Z. H., G. K. R. Angaru, L. P. Lingamdinne, J. R. Koduru, and Y.-Y. Chang (2023). Highly Efficient Cd (II) Removal from Groundwater Utilizing Layered Mixed Metal Oxides-Graphitic Carbon Nitride Composite with Improved Cycling Stability. *Journal of Water Process Engineering*, **56**; 104276

Muráth, S., N. Dvorníková, D. Moreno-Rodríguez, R. Novotnỳ, M. Pospíšil, M. Urbanová, J. Brus, and F. Kovanda (2023). Intercalation of Atorvastatin and Valsartan into MgAl Layered Double Hydroxide Host Using a Restacking Procedure. *Applied Clay Science*, **231**; 106717

Oladipo, A. A. (2021). Rapid Photocatalytic Treatment of High-Strength Olive Mill Wastewater by Sunlight and UV-Induced $CuCr_2O_4$@ CaFe–LDO. *Journal of Water Process Engineering*, **40**; 101932

Otgonbayar, Z. and W.-C. Oh (2023). Bandgap Energy Controlling of Quaternary Metal Sulfide-Graphene-ZnO Ternary Nanocomposite for Photocatalytic Reduction of CO_2. *Separation and Purification Technology*, **324**; 124522

Palapa, N. R. and A. Wijaya (2023). Layered Double Hydroxide Coated by Carbon-Based Material for Environmental Dye Pollutant. *Indonesian Journal of Material Research*, **1**(3); 84–90

Pan, C., W. Wang, Y. Zhang, J. C. Nam, F. Wu, Z. You, J. Xu, and J. Li (2023). Porous Graphitized Carbon-Supported FeOCl As a Bifunctional Adsorbent-Catalyst for the Wet Peroxide Oxidation of Chlorinated Volatile Organic Compounds: Effect of Mesopores and Mechanistic Study. *Applied Catalysis B: Environmental*, **330**; 122659

Prabhu, S., T. D. Thangadurai, P. V. Bharathy, and P. Kalugasalam (2022a). Synthesis and Characterization of Nickel Oxide Nanoparticles Using Clitoria Ternatea Flower Extract: Photocatalytic Dye Degradation under Sunlight and Antibacterial Activity Applications. *Results in Chemistry*, **4**; 100285

Prabhu, S., T. D. Thangadurai, T. Indumathi, and P. Kalugasalam (2022b). Enhanced Visible Light Induced Dye Degradation and Antibacterial Activities of ZnO/NiO Nanocomposite Synthesized Using *Clitoria ternatea* Flower Extract. *Inorganic Chemistry Communications*, **146**; 110077

Rahayua, H. A. and S. Yamtinaha (2018). Effect of Extraction Method for Mangosteen Skin (*Garcinia mangostana* L.) on the Efficiency as a Dye Sensitized Solar Cell (DSSC). page 14–27

Rohmatullaili, N. Ahmad, D. Erviana, D. Savira, R. Mohadi, and A. Lesbani (2024). Enhancing the Performance of Modified ZnAl LDH As Hybrid Catalyst-Adsorbent on Tetracycline Removal under Solar Light Irradiation. *Inorganic Chemistry Communications*, **161**; 112101

Samrot, A. V., E. N. Michael, D. A. Anand, J. L. Mercy, G. S. Sabesan, B. K. Mohanty, S. Visvanathan, and S. Saigeetha (2022). The Utilization of *Garcinia mangostana* Fibers for the Removal of Crystal Violet Dye. *Materials Today: Proceedings*, **59**; 1550–1554

Shen, J.-C., H.-Y. Zeng, C.-R. Chen, and S. Xu (2020). A Facile Fabrication of Ag_2O-Ag/ZnAl-Oxides with Enhanced Visible-Light Photocatalytic Performance for Tetracycline Degradation. *Applied Clay Science*, **185**; 105413

Silaen, L., N. R. Palapa, Elfita, R. Mohadi, and A. Lesbani (2021). Intercalated Zn-Cr-[α-$SiW_{12}O_{40}$] as Removal Agents of Cobalt (II) in Watery Phase: Adsorption and Regeneration Study. *Chiang Mai Journal of Science*, **48**(2); 545–556

Silva-Osuna, E., A. Vilchis-Nestor, R. Villarreal-Sanchez, A. Castro-Beltran, and P. Luque (2022). Study of the Optical Properties of TiO_2 Semiconductor Nanoparticles Synthesized Using Salvia Rosmarinus and Its Effect on Photocatalytic Activity. *Optical Materials*, **124**; 112039

Siregar, P. M. S. B. N., N. R. Palapa, A. Wijaya, E. S. Fitri, and A. Lesbani (2021). Structural Stability of Ni/Al Layered Double Hydroxide Supported on Graphite and Biochar toward Adsorption of Congo Red. *Science and Technology Indonesia*, **6**(2); 85–95

Song, Z., H. Gao, G. Liao, W. Zhang, and D. Wang (2022). A Novel Slag-Based Ce/TiO_2@ LDH Catalyst for Visible Light Driven Degradation of Tetracycline: Performance and Mechanism. *Journal of Alloys and Compounds*, **901**; 163525

Sun, C., Y. Wang, L. Wu, J. Hu, X. Long, H. Wu, and F. Jiao (2022). In Situ Preparation of Novel P–N Junction Photocatalyst MgAl-LDH/$(BiO)_2CO_3$ for Enhanced Photocatalytic Degradation of Tetracycline. *Materials Science in Semiconductor Processing*, **150**; 106939

Tajat, N., W. El Mouhri, W. El Hayaoui, I. Nadif, A. Idlahcen, I. Bakas, M. Badreddine, M. Tamimi, A. Assabbane, and S. Qourzal (2024). Facile Synthesis of Ag_2CO_3/Ag_2O@ NiFe LDH Nanohetrostructure with Enhanced Photocatalytic Performance for MB Dye Degradation under Visible Light Irradiation. *Colloids and Surfaces A: Physicochemical and Engineering Aspects*, **681**; 132789

Vasseghian, Y., D. Sezgin, D. C. Nguyen, H. Y. Hoang, and M. S. Yilmaz (2023). A Hybrid Nanocomposite Based on CuFe Layered Double Hydroxide Coated Graphene Oxide for Photocatalytic Degradation of Trimethoprim. *Chemosphere*, **322**; 138243

Villegas-Fuentes, A., H. Garrafa-Gálvez, R. Quevedo-Robles, M. Luque-Morales, A. Vilchis-Nestor, and P. Luque (2023). Synthesis of Semiconductor ZnO Nanoparticles Using Citrus Microcarpa Extract and the Influence of Concentration on Their Optical Properties. *Journal of Molecular Structure*, **1281**; 135067

Wang, G., D. Li, S. Wang, Z. Zhao, S. Lv, and J. Qiu (2021). Ternary NiFeMn Layered Metal Oxide (LDO) Compounds for Capacitive Deionization Defluoridation: The Unique Role of Mn. *Separation and Purification Technology*, **254**; 117667

Wang, M., J. Wang, M. Li, X. Wang, Y. Sima, and Q. Wu (2022a). Novel In_2S_3/Zn–Al LDHs Composite As an Efficient Visible-Light-Driven Photocatalyst for Tetracycline Degradation. *Optical Materials*, **128**; 112376

Wang, R., X. Ren, and W. Guo (2023a). CeO_2@ LDH Decorated 3D Porous Module with Mortise-Tenon Structure: Activation of Peroxymonosulfate for Ultrafast Removal of Tetracycline. *Journal of Cleaner Production*, **428**; 139452

Wang, Y., T. Liu, Y. Xie, N. Li, Y. Liu, J. Wen, M. Zhang, W. Feng, J. Huang, and Y. Guo (2022b). *Clitoria ternatea* Blue Petal Extract Protects against Obesity, Oxidative Stress, and Inflammation Induced by a High-Fat, High-Fructose Diet in C57BL/6 Mice. *Food Research International*, **162**; 112008

Wang, Y., X. Lu, P. Wang, S. Wu, Q. Wang, N. Hu, X. Liu, and L. Wang (2023b). In Situ Confinement of PdO within Zeolite As Robust Adsorbent/catalyst for Toluene Elimination. *Separation and Purification Technology*, **327**; 124913

Xin Lee, K., K. Shameli, M. Miyake, N. Kuwano, N. B. Bt Ahmad Khairudin, S. E. Bt Mohamad, and Y. P. Yew (2016). Green Synthesis of Gold Nanoparticles Using Aqueous Extract of *Garcinia mangostana* Fruit Peels. *Journal of Nanomaterials*, **2016**; 1–7

Xu, K., Z. Zhu, C. Hu, J. Zheng, H. Peng, and B. Liu (2023a). Fabrication of Unconventional S-Scheme NiAl LDH/$Ag_6Si_2O_7$ Heterojunction Photocatalysts: Outstanding Photocatalytic Performance and Photocatalytic Mechanism for Tetracycline Degradation. *Colloids and Surfaces A:*

Physicochemical and Engineering Aspects, **674**; 131806

Xu, X., X. Zeng, C. Zhang, R. Huang, and W. Ding (2023b). Enhanced Electrocatalytic Removal of Tetracycline Using Dual Carbon Material Combined Particle Electrodes in a Three-Dimensional Electrochemical System: Degradation Pathway and Mechanism. *Journal of Cleaner Production*, **419**; 138257

Yang, X., Y. Li, F. Kong, X. Sun, S. Wang, and Y. Cui (2022). Effect of ZnFe-LDHs Modified Oyster Shell on the Removal of Tetracyclines Antibiotics and Variation of Tet Genes in Vertical Flow Constructed Wetlands. *Chemical Engineering Journal*, **431**; 134093

Yang, Z., S. Peng, H. Wang, Z. Zhang, Y. Xu, J. Sun, Z. Xu, and G. Guo (2023). Enhanced Catalytic Activity for CO Esterification to Dimethyl Oxalate Via Increasing Lewis Basic Sites in Pd/MgAl-LDO Catalyst. *Catalysis Communications*, **184**; 106781

Yasir, B., D. Purwaningsih, N. R. Rumata, N. Wahyuddin, M. A. AR, N. Hikmah, and N. F. Rahman (2022). Application Chemometrics-Assisted Fingerprinting Profiling of Extract Variation from Mangosteen (*Garcinia mangostana* L.) Using FTIR Method. *Journal of Pharmaceutical and Medicinal Sciences*, **6**(2); 50–53

Ye, H., S. Liu, D. Yu, X. Zhou, L. Qin, C. Lai, F. Qin, M. Zhang, W. Chen, and W. Chen (2022). Regeneration Mechanism, Modification Strategy, and Environment Application of Layered Double Hydroxides: Insights Based on Memory Effect. *Coordination Chemistry Reviews*, **450**; 214253

Yuliasari, N., A. Wijaya, R. Mohadi, E. Elfita, and A. Lesbani (2022). Photocatalytic Degradation of Malachite Green by Layered Double Hydroxide Based Composites. *Bulletin of Chemical Reaction Engineering & Catalysis*, **17**(2); 240–249

Zahara, Z. A., L. Silaen, N. Normah, N. Juleanti, and N. R. Palapa (2023). Layered Double Hydroxide Zn/M^{3+} (M^{3+}= Al and Cr) as Highly Efficient Adsorbent of Heavy Metal Pb (II). *Indonesian Journal of Material Research*, **1**(1); 8–14

Zheng, X., Y. Dong, and Q. Zhu (2020). Enhanced Photocatalysis of MgAl Layered Double Oxide Nanosheets with B, N-Codoped Carbon Coating for Tetracycline Removal. *Applied Clay Science*, **193**; 105694

Zhu, J., J. Wang, J. He, and L. Hu (2023). Fabrication of CdS/ZnCr-LDH Heterojunctions with Enhanced of Tetracycline Hydrochloride Photocatalytic Degradation under Visible Light. *Optical Materials*, **136**; 113456

